ARMY RESEARCH LABORATORY

Nanoengineering Applied to Tungsten

**by Q. Wei, B. E. Schuster, L. J. Kecskes, R. J. Dowding,
K. C. Cho, L. S. Magness, E. Ma, K. T. Ramesh, and R. Z. Valiev**

ARL-RP-123 **May 2006**

A reprint from the *Proceedings of the Sixth International Conference on Tungsten, Refractory & Hardmetals*, sponsored by the Metal Powder Industries Federation in cooperation with the Refractory Metals Association and APMI International, pp. 216–225, 7–8 February 2006, Sheraton World Resort, Orlando, FL.

Reprinted with permission from *Tungsten, Refractory & Hardmentals VI*, Metal Powder Industries Federation 105 College Road East, Princeton, NJ, 2006.

NOTICES

Disclaimers

The findings in this report are not to be construed as an official Department of the Army position unless so designated by other authorized documents.

Citation of manufacturer's or trade names does not constitute an official endorsement or approval of the use thereof.

Destroy this report when it is no longer needed. Do not return it to the originator.

Army Research Laboratory
Aberdeen Proving Ground, MD 21005-5066

ARL-RP-123 **May 2006**

Nanoengineering Applied to Tungsten

Q. Wei
University of North Carolina-Charlotte

B. E. Schuster, L. J. Kecskes, R. J. Dowding, and K. C. Cho, L. S. Magness
Weapons and Materials Research Directorate, ARL

E. Ma and K. T. Ramesh
The Johns Hopkins University

R. Z. Valiev
Ufa State Aviation Technical University

A reprint from the *Proceedings of the Sixth International Conference on Tungsten, Refractory & Hardmetals*, sponsored by the Metal Powder Industries Federation in cooperation with the Refractory Metals Association and APMI International, pp. 216–225, 7–8 February 2006, Sheraton World Resort, Orlando, FL.

Reprinted with permission from *Tungsten, Refractory & Hardmentals VI*, Metal Powder Industries Federation 105 College Road East, Princeton, NJ, 2006.

REPORT DOCUMENTATION PAGE

Form Approved
OMB No. 0704-0188

1. REPORT DATE *(DD-MM-YYYY)*	2. REPORT TYPE	3. DATES COVERED (From - To)
May 2006	Reprint	September 2004–September 2005

4. TITLE AND SUBTITLE
Nanoengineering Applied to Tungsten

5a. CONTRACT NUMBER

5b. GRANT NUMBER

5c. PROGRAM ELEMENT NUMBER

6. AUTHOR(S)
Q. Wei,[*] B. E. Schuster, L. J. Kecskes, R. J. Dowding, K. C. Cho, L. S. Magness, E. Ma, [†] K. T. Ramesh,[†] and R. Z. Valiev[††]

5d. PROJECT NUMBER
58T8G7

5e. TASK NUMBER

5f. WORK UNIT NUMBER

7. PERFORMING ORGANIZATION NAME(S) AND ADDRESS(ES)
U.S. Army Research Laboratory
ATTN: AMSRD-ARL-WM-TC
Aberdeen Proving Ground, MD 21005-5066

8. PERFORMING ORGANIZATION REPORT NUMBER
ARL-RP-123

9. SPONSORING/MONITORING AGENCY NAME(S) AND ADDRESS(ES)

10. SPONSOR/MONITOR'S ACRONYM(S)

11. SPONSOR/MONITOR'S REPORT NUMBER(S)

12. DISTRIBUTION/AVAILABILITY STATEMENT
Approved for public release; distribution is unlimited.

13. SUPPLEMENTARY NOTES
A reprint from the *Proceedings of the Sixth International Conference on Tungsten, Refractory & Hardmetals*, sponsored by the Metal Powder Industries Federation in cooperation with the Refractory Metals Association and APMI International, pp. 216–225, 7–8 February 2006, Sheraton World Resort, Orlando, FL.
*Department of Mechanical Engineering, University of North Carolina-Charlotte, 9201 University City Blvd., Charlotte, NC 28223
†Center for Advanced Ceramic and Metallic Systems (CAMCS), the Johns Hopkins University, Baltimore, MD 21818
††Ufa State Aviation Technical University, Ufa 450000, Russia

14. ABSTRACT
We have investigated the microstructure and mechanical properties of fully dense tungsten with ultrafine-grained (UFG) and nanocrystalline (NC) microstructure. The UFG/NC tungsten was processed by severe plastic deformation at low homologous temperatures (T/T_m). To obtain the UFG microstructure, a combination of equal channel angular pressing at relatively high temperatures followed by rolling at lower temperatures was employed, which resulted in an average grain size of ~500 nm. To obtain the nanocrystalline microstructure (grain size ~100 nm and below), high-pressure torsion was utilized. Our experimental results show that the UFG/NC microstructures not only significantly elevate the strength of tungsten, they also re-instate its ductility, decrease its strain rate sensitivity, and reduce its work hardening capability. These factors work together to greatly enhance the susceptibility of tungsten to adiabatic localization under uni-axial dynamic loading.

15. SUBJECT TERMS
tungsten, nanoengineering, microstructure, ultrafine-grained, nanocrystalline

16. SECURITY CLASSIFICATION OF:			17. LIMITATION OF ABSTRACT	18. NUMBER OF PAGES	19a. NAME OF RESPONSIBLE PERSON
a. REPORT	b. ABSTRACT	c. THIS PAGE			Brian E. Schuster
UNCLASSIFIED	UNCLASSIFIED	UNCLASSIFIED	UL	16	19b. TELEPHONE NUMBER (*Include area code*) 410-278-6733

NANOENGINEERING APPLIED TO TUNGSTEN

Q. Wei[1,2], B. E. Schuster[2,3], L. J. Kecskes[3], R. J. Dowding[3], K. C. Cho[3], L. S. Magness[3], E. Ma[2], K. T. Ramesh[2] and R. Z. Valiev[4]

[1]Department of Mechanical Engineering, University of North Carolina-Charlotte, 9201 University City Blvd., Charlotte, NC 28223

[2]Center for Advanced Ceramic and Metallic Systems (CAMCS), the Johns Hopkins University, Baltimore, MD 21818

[3]US Army Research Laboratory, Aberdeen Proving Ground, MD 21005

[4]Ufa State Aviation Technical University, Ufa 450000, Russia

ABSTRACT

We have investigated the microstructure and mechanical properties of fully dense tungsten with ultrafine-grained (UFG) and nanocrystalline (NC) microstructure. The UFG/NC tungsten was processed by severe plastic deformation at low homologous temperatures (T/T_m). To obtain the UFG microstructure, a combination of equal channel angular pressing at relatively high temperatures followed by rolling at lower temperatures was employed, which resulted in an average grain size of ~500 nm. To obtain the nanocrystalline microstructure (grain size ~100 nm and below), high-pressure torsion was utilized. Our experimental results show that the UFG/NC microstructures not only significantly elevate the strength of tungsten, they also re-instate its ductility, decrease its strain rate sensitivity, and reduce its work hardening capability. These factors work together to greatly enhance the susceptibility of tungsten to adiabatic shear localization under uni-axial dynamic loading.

INTRODUCTION

Metals and alloys with grain size in the ultrafine grained (UFG, grain size d smaller than 500 nm but greater than 100 nm) and nanocrystalline (NC, d<100 nm) have drawn much interest in the past two decades due to their desirable properties[1-4]. Of particular interest is their much elevated strength compared to the coarse grained (CG) counterparts. However, a general observation accompanying such high strength is the loss of ductility, especially under tensile loading[5-7]. It is only until recently that it is recognized the loss of ductility of UFG/NC metals is an artificial defect induced phenomenon, instead of an intrinsic property of UFG/NC metals[8-12]. The focuses of investigations has shifted recently to other unusual properties of UFG/NC metals and alloys, including the retained ductility with some special processing routes[8-10, 12]. The most direct cause of the loss of ductility is the introduction of volume defects such as residual porosity, poor inter-particle bonding due to impurity contamination, etc[13]. These effects are a consequence of so called "two-step" processing where UFG/NC powders are produced followed by hot compaction. One strategy employed to mitigate such detrimental effects is "one-step" processing where handling of powders in open air is avoided, or the starting material is in fully dense, bulk forms. Koch and his co-workers have demonstrated that NC Cu with grain size around 20 nm produced by "in-situ consolidation" in a ball milling vial can have very significant plastic deformation

before failure under tension (tensile strain >10%)[9]. Another technique for the production of UFG/NC metals is severe plastic deformation (SPD) where a fully dense bulk work piece is subjected to very large amounts of plastic strain[14]. This technique avoids the handling of powders and subsequent consolidation, and is therefore a one-step process. Very recently, a bi-modal grain size distribution in Cu has also been applied to the production of strong and ductile microstructures where the NC grains provide the strengthening mechanism and the relatively large (d a few microns) grains accommodate the plasticity[11, 12]. This "microstructure engineering" concept has since been used in other systems[3].

The majority of efforts on UFG/NC metals are on those with face-centered-cubic (FCC) structures such as Al, Cu, Ni, etc[15]. Much less work has been conducted on body-centered-cubic (BCC) metals. One reason for this lack of balance resides with the difficulty in refining the grain size of BCC metals into the UFG/NC regimes. Recent efforts have shown that UFG/NC BCC metals have some very unique behavior in comparison to the FCC counterparts[16-26]. For example, UFG/NC Fe exhibits localized shearing even under quasi-static uni-axial compression[16, 27, 28]. NC vanadium fails in a manner similar to metallic glasses under dynamic uni-axial compression[19]. Such observations have been explained on the basis of the vanishing strain hardening and a much reduced strain rate sensitivity (SRS). As is known, such a deformation and failure mode is desirable for a kinetic energy penetrator material. There has been tremendous research work in search of a replacement for depleted uranium (DU) for the making of such penetrators, and among all the candidates, W, a BCC metal, seems to be the best in terms of its high mass density which rivals that of DU[29].

BCC metals are known to be much more vulnerable to soluble interstitial impurities, which have been held responsible for its brittle failure at low homologous temperatures[30]. Tungsten the most notorious with an extremely high susceptibility to impurity attack. Conventional, powder metallurgy (PM) produced CG W exhibits a very high ductile-to-brittle transition temperature (DBTT around 150°C)[31]. Efforts to produce UFG/NC W through PM technology have had little success to this point. Very recently, we have shown that SPD may be an alternative way for grain size reduction to produce UFG/NC W[22, 23]. In this paper, we report and review the application of "nano-engineering" in the context of "grain-boundary engineering" to W with commercial purity.

EXPERIMENTAL PROCEDURES

In this work, we use severe plastic deformation (SPD)[14] for the grain size reduction of commercial purity W. There are a number of variants of SPD technique. First, we use the equal-channel-angular-press (ECAP) and ECAP followed by low temperature rolling for the production of UFG W. Details of ECAP can be found in numerous papers, e.g. [14]. In this technique, the work piece is pushed through two connecting channels with the same cross-sectional area. If the connecting angle between the two channels is 90 degrees, the work piece will experience an equivalent strain of ~1.1. The recrystallization temperature of W is around 1250°C[30]. In this work, to ensure the efficiency of grain size reduction the ECAP was performed at 1000°C. To alleviate oxidation of the W work piece, the W rod was encapsulated in a stainless steel canister. The die angle (or connecting angle between the channels) is 120 degrees to avoid cracking of the work piece. Another SPD technique we used to reduce the grain size of W is high-pressure torsion (HPT)[14, 32]. In this technique, a disk of W (~10 mm in diameter and ~1.0 mm in thickness) is subjected to a high pressure (~6 GPa) while a torsion is applied to it. This technique allows one to pump a tremendous amount of plastic strain at the edge of the disk (after one complete turn the equivalent strain is ~18 at the edge of the disk with the above dimension). In this work, HPT was conducted at 500°C, much lower than the recrystallization temperature of W.

Microstructures of the processed materials were analyzed using optical microscopy, scanning electron microscopy (SEM), and transmission electron microscopy (TEM). SEM is used to examine the post-loading specimen surface to identify the deformation and failure mechanisms. TEM, both diffraction contrast and phase contrast (high-resolution lattice imaging) is used to analyze grain size, defects and their distributions, and grain boundary structure.

The processed W was tested under both uni-axial quasi-static compression (strain rate 10^{-4} s^{-1} to 10^{0} s^{-1}) and dynamic compression (using the Kolsky bar or split-Hopkinson pressure bar (SHPB) technique, strain rate ~10^{3} s^{-1})[33]. For the HPT processed W, due to the limited dimension of the disk, we used a miniaturized SHPB system (desk-top Kolsky bar, or DTKB)[34] to obtain the dynamic data. Figure 1 displays a schematic of such a DTKB system, and some detailed description about the system. To observe the initiation and evolution of adiabatic shear bands (ASBs), we used a high speed camera (DRS Hadland Ultra 8, maximum framing rate 10^{8} fps) which was synchronized with the Kolsky bar system to record a movie.

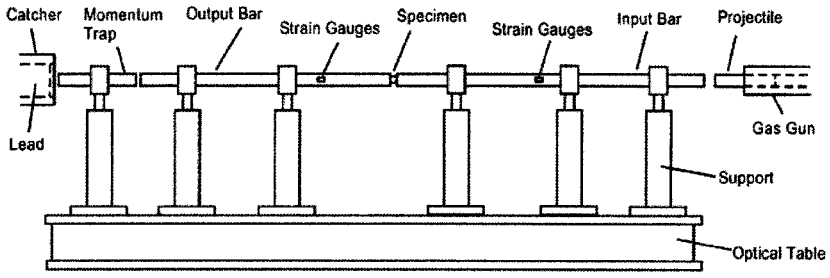

Figure 1 Schematic of the desk-top Kolsky bar system. The bars and their many supports are seated on a precision optical table (2 feet in length). The bars are made of high strength maraging steel. The diameter of the bars is ~3.18 mm. The specimen is sandwiched between the input and the output bar. Due to the unusual high strength of the HPT W, impedance matched WC platens shrink fitted into Ti-6Al-4V collars were used to protect the input and output bars. Thus the specimen is first sandwiched between the WC platens and then mounted between the two bars.

RESULTS AND DISCUSSION

First, we will present results of microstructure observations, followed by mechanical testing results n. This is followed by observations of deformation and failure mechanisms. The results will be discussed in connection with a mechanistic model of ASBs.

Figure 2 (a) shows the optical microstructure of W after four passes of ECAP at 1000°C. It is to be noted here that the starting material has a grain size in the range of a few tens of micrometers. Grain size reduction via ECAP is obvious. However, ECAP at 1000°C can only refine the grain size of W down to a few micrometers due to dynamic recrystallization and grain growth at this temperature. To further refine the grain size, the ECAP W was rolled at 800°C and below. Figure 2 (b) displays the TEM micrograph of W that was further rolled at 600°C to an additional equivalent strain of 1.8. The average grain size (or subgrain size, since a large population of the grain boundaries are of low angle type, as suggested by selected area diffraction (SAD, not shown here)) is around 500 nm, thus in the UFG regime.

HPT results in much smaller grain size, and most of the grain boundaries are of large angle type. Figure 3 (a) displays a typical microstructure of HPT W. The average grain size as derived from TEM analyses is about 100 nm. XRD line broadening analyses resulted in a much smaller grain size value (~40 nm). This discrepancy is primarily due to the heavily defected grains in the HPT W. Defects such as dislocations and other coherent domains (sub-grain boundaries) all contribute to broadening the XRD peaks, which leads to a much smaller apparent grain size. The SAD pattern (Fig. 3 (b)) shows almost continuous rings, indicating absence of texturing. Fig. 3 (c) is a typical HRTEM image of a large angle grain boundary. A few interesting characters can be identified with this grain boundary. First, it is of large angle type. It has a number of atomic facets, steps or ledges, suggesting its high energy and non-equilibrium nature[35-37]. Third, no grain boundary phase, amorphous or crystalline, can be associated with the grain boundary. In other words, the crystalline structure of the constituent grains is disrupted only by the presence of the grain boundary, and the grain boundary is clean, and well defined. HRTEM of the same specimen also reveals the existence of a large number of edge dislocations in the vicinity of the grain boundary. This is unusual since plasticity of W at such low temperature is usually accommodated

by screws by means of the well-known double kink mechanism, and only straight screws are observed by TEM after finite plastic deformation[38].

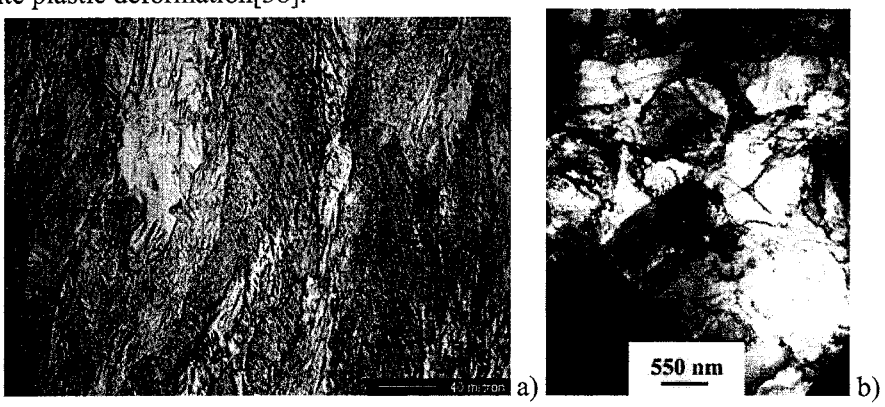

Figure 2 Optical micrograph of ECAP W (a) (4 passes at 1000°C) showing refined microstructure due to severe plastic deformation. Notice that the pre-existing grain boundaries are still visible. After further rolling at relatively low temperature, the microstructure is refined into the UFG regime (b). However, selected area diffraction pattern (not shown here) indicates that many grain boundaries are of the low angle type.

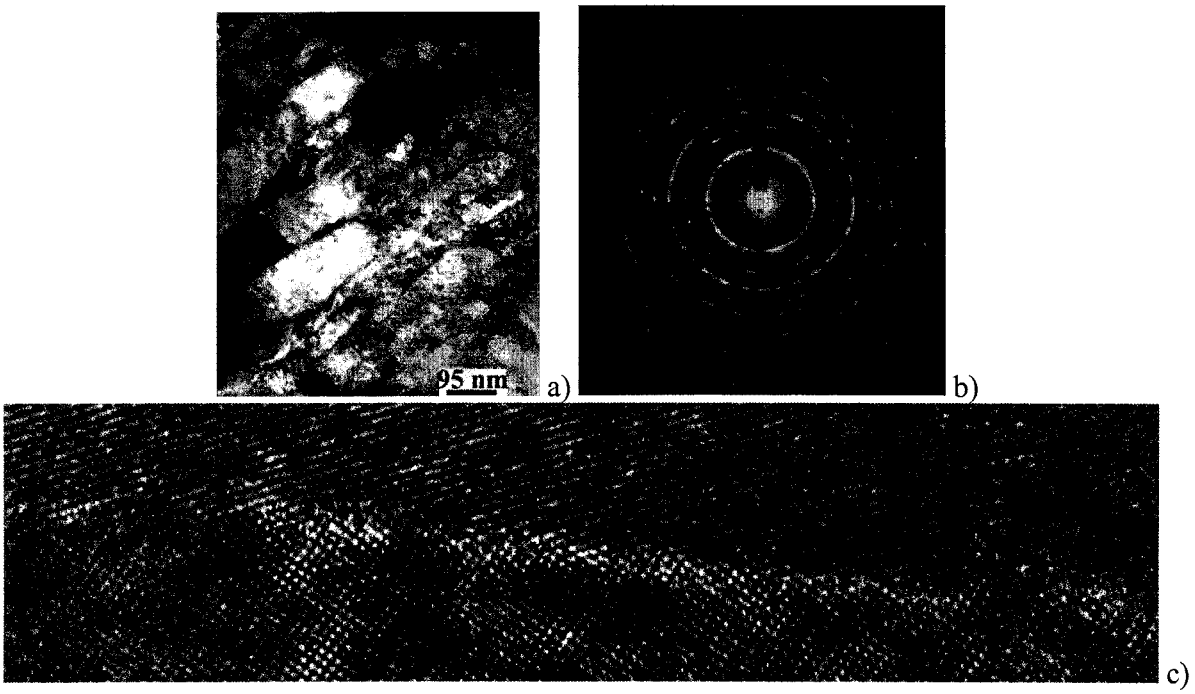

Figure 3 (a) Bright field TEM image showing the nanocrystalline microstructure of HPT W. (b) Selected area diffraction pattern indicates continuous rings and apparent absence of texturing. (c) Lattice image of a grain boundary in the HPT W showing large angle GB with atomic ledges and steps, suggesting its high energy and non-equilibrium nature.

Figure 4 (a) shows the quasi-static and dynamic stress-strain curves of W specimens processed by ECAP and ECAP+rolling (will be referred to henceforth as ECAP+R W). Since the control sample (CG conventional W) has been widely investigated[39, 40], and our results are close to those in the literature, they will not be presented here. The following observations can be derived from the stress-strain curves. First, ECAP at 1000°C (6 passes) has increased the quasi-static strength to 1.5 times that of the control sample (apparent yield strength of CG W is ~1.0 GPa). Further low temperature rolling has increased the

strength to nearly twice its CG value. Another observation is the much reduced work hardening in the SPD processed W. Under dynamic compression, SPD W shows flow softening at quite small plastic strains, in sharp contrast to the CG W where under dynamic loading slight hardening is observed. This flow softening, especially in the ECAP+R W, is due to a change in deformation mode, as detailed later in this paper.

Microhardness measurement on the HPT W shows that the nano-W is super-strong with a hardness value around 11 GPa at the rim of the disk. This hardness value is remarkable even when compared with some strong ceramics (E.g., the hardness of sintered Si_3N_4 ceramic is about 20 GPa[41]). Quasi-static compression of the HPT W showed a yield strength about 3.5 GPa, in accordance with the hardness value if the Tabor relation[42] between Vicker's hardness and yield strength of a isotropic materials is assumed. Figure 4 (b) displays a few dynamic stress strain curves of HPT W. The most salient feature in these curves is the very early precipitous stress collapse, which is one of the most desirable properties for a penetrator material. Later in this paper, we will show that such stress collapse is a consequence of plastic deformation mechanism transition from uniform mode to localized ASB.

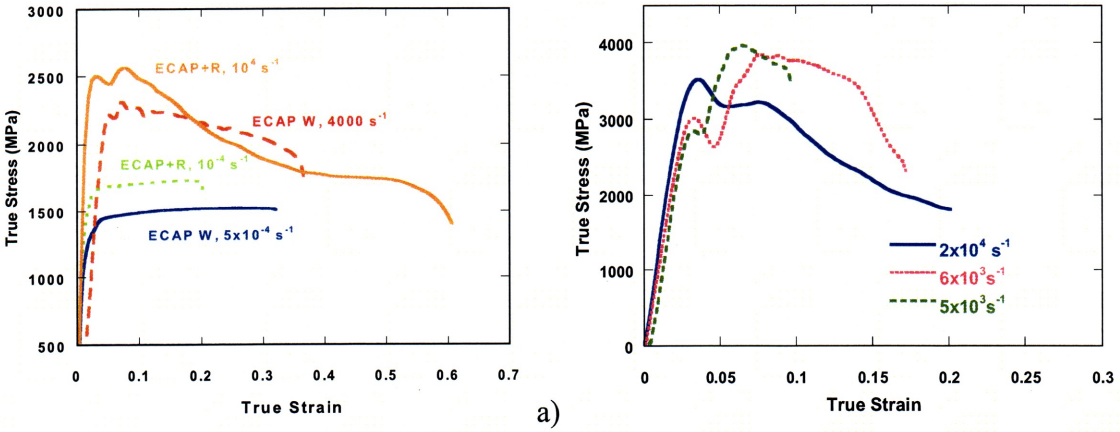

Figure 4 (a) True stress-strain curves of ECAP W and ECAP+R W under quasi-static and dynamic uni-axial compression. The significant flow softening in the ECAP+R W is of particular interest. (b) Dynamic stress-strain curves of HPT W as measured by desk-top Kolsky bar technique. HPT W exhibits much more elevated flow strength with much earlier stress collapse compared to the ECAP+R W.

Under uni-axial quasi-static and dynamic compression, conventional CG W, and extruded W (extrusion at 1200°C) that shows strength levels close to the ECAP W in this paper exhibits axial cracks (cracks parallel to the loading axis)[39]. Our ECAP W exhibits similar features under uni-axial loading[23]. Most of the cracks are along the pre-existing grain boundaries, consistent to tensile behavior of such W where failure occurs at a stress level about only half that of compression, and with no evidence of plastic deformation. The failure mode is similar to that of most ceramics.

Figure 5 (a) shows the post-loading (uni-axial dynamic compression) optical micrograph of an ECAP+R W, with the corresponding stress-strain response shown in Fig. 4 (a). Instead of almost uniformly distributed axial cracks, clear evidence of shear bands is observed. Higher magnification SEM imaging (Figure 5 (b), for example) indicates severe and localized adiabatic shear flow within the ASBs. Polishing of the roughened surface followed by chemical etching revealed the detailed microstructure of the shear bands, including density and direction of the shear lines, width of the shear bands (around 40 μm in the UFG W), and cracking along the central line (or middle line) of the shear bands (Fig. 5 (b)). High-speed photography (not shown here) indicates that the stress-collapse in the stress-strain curves roughly corresponds to the initiation of ASBs[23]. The strain level at which ASBs develop is around 0.1 (10%), and they are fully developed at a strain level of ~15%. On-set of secondary shear bands was also observed via high-speed photography.

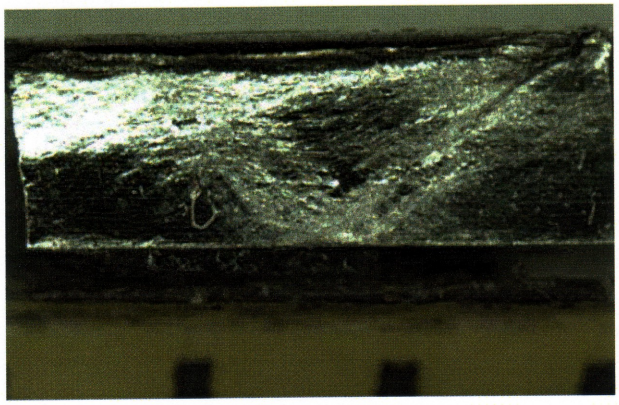
a)
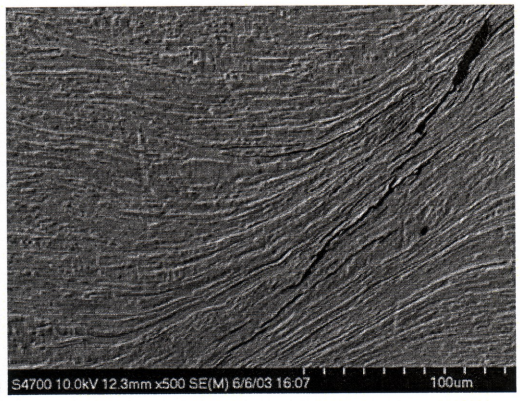

b)

Figure 5 (a) Optical micrograph of post-loading (uni-axial dynamic compression) ECAP+R W showing the ASBs. Loading is vertical in this figure. Each division corresponding to the dark markers at the bottom of the image is 1 mm. (b) SEM showing the severe and highly localized flow in the ASB. The roughened surface has been polished and etched using a standard Murakami solution to reveal the microstructure of the ASB.

Figure 6 (a) shows a post-loading (desk-top Kolsky bar) optical micrograph of the HPT nano-W. Again, in stead of axial cracking, we observe a localized shear band at an angle of ~45 degrees with respect to the loading direction (horizontal in this case). SEM micrograph of Figure 6 (b) shows the severe curving of the pre-existing scratches which were introduced during specimen preparation prior to dynamic loading. In this case, the shear band width (about 5 μm) is much smaller compared to that of the UFG W specimens. In other UFG/NC BCC metals such as Fe, change of shear band width with grain size is also observed, and the underlying mechanism is still under investigation. Figure 6 (b) also shows the crack as a consequence of highly localized adiabatic shearing.

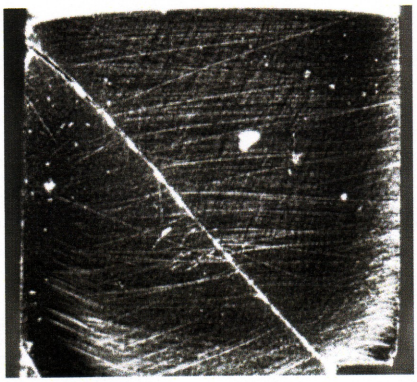
a)
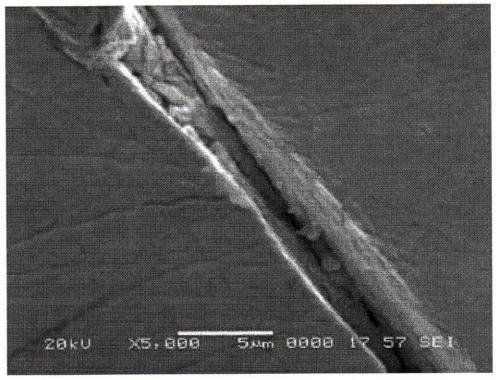

b)

Figure 6 (a) Optical image of a post-loading (desk-top Kolsky bar) HPT nano-W showing a single shear band. The loading is horizontal. (b) SEM image showing severe curving of the pre-existing scratches approaching the shear band. The crack is a result of severe and highly concentrated shear flow within the shear band.

Because of their high mass density, tungsten and tungsten heavy alloys (WHA) have been investigated extensively for the production of kinetic energy anti-armor penetrators in place of depleted uranium (DU). However, most of the efforts have failed, mainly due to the lack of plasticity of conventional CG W. Plastic deformation is needed to introduce adiabatic heating that is the pre-requisite for the development of ASB. On the other hand, uniform plastic deformation of the penetrator material is to be avoided so that the kinetic energy can be used for penetration. It is well known that uniform plastic deformation of the penetrator material is the cause for "mushrooming" of the penetrator head, in contrast to "self-sharpening" where the penetrator head remains sharp and failed penetrator material is discarded

away via adiabatic shearing, thus leaving a small penetration channel within the target. The self-sharpening effect of the penetrator is rooted in the material property in that under dynamic loading, the plastic deformation is highly concentrated in a narrow region[29].

It has been recognized that the soluble interstitial impurities such as C, N, S, etc. are responsible for the ceramic like behavior of CG conventional W[30]. These impurities segregate along the grain boundaries (GBs) to render the GBs the weak links under mechanical straining. However, brittle behavior is not intrinsic to W, at least not so at relatively high temperatures, since experimental results have shown that single crystal tungsten can be deformed to significant plastic strain under tension even at liquid nitrogen temperature[43]. Therefore, if the pre-existing malignant impurities can somehow be depleted, one should expect improved ductility. One strategy to furnish this is by means of "grain boundary engineering"[44]. If more grain boundaries are created in addition to the pre-existing grain boundaries, and if appropriate kinetic condition is provided for the pre-existing GB impurities to diffuse away from the pre-existing GBs and be relocated to the newly created GBs, the average impurity concentration at the GBs can be reduced. This will increase the grain boundary strength and reinstate the ductility. The most efficient way to induce more GBs without worsening impurity contamination is the SPD technique. It has been borne out that the GBs induced by SPD have some special properties[37]. For instance, they are of non-equilibrium and high energy nature. Such GBs are ideal hosting sites for interstitial impurities. It has also been proposed that the peculiar nature of the SPD induced GBs explains the paradox of many UFG/NC metals where significant ductility is observed concurrently with much elevated strength[45].

Another contributing factor to the re-instated ductility of the SPD W might be the high density of edge dislocations as observed in HRTEM in the vicinity of the GBs. Systematic work by Gumbsch, et al. [46] on the controlling factors for the fracture toughness and brittle-to-ductile transition in single crystal W indicates that pre-plastic-deformation of the specimen can increase both low and high temperature fracture toughness. Particularly, much improved high temperature fracture toughness has been achieved by pre-plastic-deformation. They pointed out that if a dislocation (either one that is generated at the crack tip or a pre-existing one) moves in the stress field along the crack tip, it will generate dislocation segments of non-screw (and thus highly mobile) character parallel to the crack tip. Our high-resolution TEM shows residual edge dislocations in the HPT nano-W. Such edges may work together with other pre-existing dislocations that are highly mobile so as to provide highly efficient shielding of the crack tip, thus resulting in relatively ductile failure.

Finally, we need to explain the enhanced propensity for ASB in SPD UFG/NC W, as evidenced in this work. Many mechanistic models have been articulated to predict the propensity of metals and alloys for ASB. One simple criterion has been proposed by Wright as[47]

$$\frac{\chi_{SB}}{a/m} = \min\left\{1, \frac{1}{(n/m)+\sqrt{n/m}}\right\}, \qquad (1)$$

where χ_{SB} is the susceptibility to ASB, a the non-dimensional thermal softening parameter defined by $a = (-\partial\sigma/\partial T)/\rho c$ (σ is the flow stress, T the temperature, ρ the density and c the specific heat of the material), n the strain hardening exponent and m the strain rate sensitivity. For a perfectly plastic material (no strain hardening) such as the SPD processed W in this work, the susceptibility reduces to

$$\chi_{SB} = \frac{a}{m} = \frac{\lambda\sigma_0}{\rho c m}, \qquad (2)$$

where $\lambda = -(1/\hat{\sigma}_0)\partial\sigma/\partial T$ is the thermal softening parameter evaluated under isothermal conditions ($\hat{\sigma}_0$ is a normalizing stress), and σ_0 is the yield strength. UFG/NC metals have much higher yield strength than their CG counterparts (the well-known Hall-Petch strengthening mechanism). Recent experimental results and theoretical analyses on the strain rate sensitivity of UFG/NC BCC metals have shown that SRS is considerably reduced in comparison to the CG microstructure[20]. A simple calculation based on the

experimental results and the physical properties of W shows that susceptibility to ASB of the UFG and NC W is several orders of magnitude higher than that of conventional CG W.

CONCLUSIONS

We have applied "nano-engineering" to produce W with some unusual microstructure characteristics and mechanical behavior. Ultrafine grained W and nanocrystalline W were processed using severe plastic deformation under various conditions. Mechanical testing under uni-axial dynamic loading showed that such UFG and NC W exhibit the long sought-after localized shearing, in stead of uniform plastic deformation and/or axial cracking. A simple model is used to explain the experimental results.

ACKNOWLEDGMENTS

The authors thank Drs. Tong Jiao, Haitao Zhang and Yulong Li for experimental assistance. They are also grateful to Drs. T. W. Wright and J. W. McCauley (Army Research Laboratory) for illuminating discussions. This work was sponsored by ARL through JHU-CAMCS under the ARMAC-RTP Cooperative Agreement #DAAD19-01-2-0003.

REFERENCES

[1] C. C. Koch, *Nanostructured materials: processing, properties and potential applications.* Norwich: Noyes Publications, 2002.

[2] M. A. Meyers, A. Mishra, and D. J. Benson, "Mechanical properties of nanocrystalline materials," *Progress in Materials Science*, vol. 51, pp. In press, 2006.

[3] D. B. Witkin and E. J. Lavernia, "Synthesis and mechanical behavior of nanostructured materials via cryomilling," *Progress in Materials Science*, vol. 51, pp. 1-60., 2006.

[4] W. W. Milligan, "Mechanical behavior of bulk nanocrystalline and ultrafine-grain metals," in *Comprehensive Structural Integrity*, vol. 8, *Interfacial and Nanoscale Fracture*, I. Milne, R. O. Ritchie, and B. Karihaloo, Eds. Amsterdam-Boston: Elsevier-Pergamon, 2003, pp. 529-550.

[5] C. C. Koch, "Optimization of strength and ductility in nanocrystalline and ultrafine grained metals," *Scripta Materialia*, vol. 49, pp. 657-662, 2003.

[6] E. Ma, "Instabilities and ductility of nanocrystalline and ultrafine-grained metals," *Scripta Materialia*, vol. 49, pp. 663-668, 2003.

[7] E. Ma, "Controlling plastic instability," *Nature Materials*, vol. 2, pp. 7-8., 2003.

[8] K. M. Youssef, R. O. Scattergood, K. L. Murty, and C. C. Koch, "Ultratough nanocrystalline copper with a narrow grain size distribution," *Applied physics letters*, vol. 85, pp. 929-931., 2004.

[9] K. M. Youssef, R. O. Scattergood, K. L. Murty, J. A. Horton, and C. C. Koch, "Ultrahigh strength and high ductility of bulk nanocrystalline copper," *Applied physics letters*, vol. 87, pp. 091904, 2005.

[10] S. Cheng, E. Ma, Y. M. Wang, L. J. Kecskes, K. M. Youssef, C. C. Koch, U. P. Trociewitz, and K. Han, "Tensile properties of in situ consolidated nanocrystalline Cu," *Acta Materialia*, vol. 53, pp. 1521-1533., 2005.

[11] Y. M. Wang and E. Ma, "Three strategies to achieve uniform tensile deformation in a nanostructured metal," *Acta Materialia*, vol. 52, pp. 1699-1709., 2004.

[12] Y. M. Wang, M. W. Chen, F. H. Zhou, and E. Ma, "High tensile ductility in a nanostructured metal," *Nature*, vol. 419, pp. 912-915, 2002.

[13] C. C. Koch and J. Narayan, "The inverse Hall-Petch effect-Fact or Artifact?," presented at Structure and mechanical properties of nanophase materials-theory and computer simulations v.s. experiments, Boston, MA, USA, 2001.

[14] R. Z. Valiev, R. K. Islamgaliev, and I. V. Alexandrov, "Bulk nanostructured materials from severe plastic deformation," *Progress in Materials Science*, vol. 45, pp. 103-189, 2000.

[15] K. S. Kumar, H. Van Swygenhoven, and S. Suresh, "Mechanical Behavior of nanocrystalline metals and alloys," *Acta Materialia*, vol. 51, pp. 5743-5774, 2003.
[16] Q. Wei, D. Jia, K. T. Ramesh, and E. Ma, "Evolution and microstructure of shear bands in nanostructured Fe," *Applied physics letters*, vol. 81, pp. 1240-1242, 2002.
[17] Q. Wei, T. Jiao, S. N. Mathaudhu, E. Ma, K. T. Hartwig, and K. T. Ramesh, "Microstructure and mechanical properties of tantalum after equal channel angular extrusion (ECAE)," *Materials science and engineering A*, vol. 358, pp. 266-272, 2003.
[18] Q. Wei, L. J. Kecskes, T. Jiao, K. T. Hartwig, K. T. Ramesh, and E. Ma, "Adiabatic shear banding in ultrafine grained Fe processed by severe plastic deformation," *Acta materialia*, vol. 52, pp. 1859-1869, 2004.
[19] Q. Wei, T. Jiao, K. T. Ramesh, and E. Ma, "Nano-structured vanadium: processing and mechanical properties under quasi-static and dynamic compression," *Scripta materialia*, vol. 50, pp. 359-364, 2004.
[20] Q. Wei, S. Cheng, K. T. Ramesh, and E. Ma, "Effect of nanocrystalline and ultrafine grain sizes on the strain rate sensitivity and activation volume: fcc versus bcc metals," *Materials science and engineering A*, vol. 381, pp. 71-79, 2004.
[21] Y. J. Wei and L. Anand, "Grain boundary sliding and separation in polycrystalline metals: application to nanocrystalline fcc metals," *Journal of the Mechanics and Physics of Solids*, vol. 52, pp. 2584-2616., 2004.
[22] Q. Wei, K. T. Ramesh, E. Ma, L. J. Kesckes, R. J. Dowding, V. U. Kazykhanov, and R. Z. Valiev, "Plastic flow localization in bulk-tungsten with ultrafine microstructure," *Applied physics letters*, vol. 86, pp. 101907, 2005.
[23] Q. Wei, T. Jiao, K. T. Ramesh, E. Ma, L. J. Kecskes, L. Magness, R. J. Dowding, V. U. Kazykhanov, and R. Z. Valiev, "Mechanical behavior and dynamic failure of high-strength ultrafine grained tungsten under uniaxial compression," *Acta Materialia*, vol. 54, pp. 77-87, 2006.
[24] T. R. Malow and C. C. Koch, "Mechanical properties in tension of mechanically attrited nanocrystalline iron by the use of miniaturized disk bend test," *Acta materialia*, vol. 46, pp. 6459-6473, 1998.
[25] T. R. Malow, C. C. Koch, P. Q. Miraglia, and K. L. Murty, "Compressive mechanical behavior of nanocrystalline Fe investigated with an automated ball indentation technique," *Materials Science and Engineering A*, vol. 252, pp. 36-43., 1998.
[26] J. E. Carsley, A. Fisher, W. W. Milligan, and E. C. Aifantis, "Mechanical behavior of bulk nanostructured iron alloy," *Metallurgical and Materials Transactions A*, vol. 29A, pp. 2261-2271, 1998.
[27] D. Jia, K. T. Ramesh, and E. Ma, "Failure mode and dynamic behavior of nanophase iron under compression," *Scripta Materialia*, vol. 42, pp. 73-78., 2000.
[28] D. Jia, K. T. Ramesh, and E. Ma, "Effects of nanocrystalline and ultrafine grain sizes on constitutive behavior and shear bands in iron," *Acta materialia*, vol. 51, pp. 3495-3590, 2003.
[29] L. S. Magness, "An overview of the penetration performances of tungsten and depleted uranium alloy penetrators: ballistic performances and metallographic examinations," presented at 20th International Symposium on Ballistics, Orlando, Florida, 2002.
[30] E. Lassner and W.-D. Schubert, *Tungsten-Properties, Chemistry, Technology of the element, allys and chemical compounds.*: Kluwer-Academic/Plenum Publishers, 1998.
[31] B. C. Allen, D. J. Maykuth, and R. I. Jaffee, "The recrystallization and ductile-brittle transition behavior of tungsten," *Journal of the institute of metals*, vol. 90, pp. 120-128, 1961.
[32] A. P. Zhilyaev, G. V. Nurislamova, B.-K. Kim, M. D. Baro, J. A. Szpunar, and T. G. Langdon, "Experimental parameters influencing grain refinement and microstructural evolution during high-pressure torsion," *Acta Materialia*, vol. 51, pp. 753-765, 2003.
[33] P. S. Follansbee, "High strain rate compression testing," in *ASM Metals Handbook*, vol. 8: American Society of Metals, 1985, pp. 190.

[34] D. Jia and K. T. Ramesh, "A rigorous assessment of the benefits of miniaturization in the Kolsky bar system," *Experimental Mechanics*, vol. 44, pp. 445-454, 2004.
[35] R. Z. Valiev, V. Y. Gertsman, and R. Kaibyshev, "Grain Boundary Structure and Properties under External Influence," *Physica Status Solidi A*, vol. 97, pp. 11-56, 1986.
[36] R. Z. Valiev, "Nanomaterial advantage," *Nature*, vol. 419, pp. 887-889., 2002.
[37] A. A. Nazarov, A. E. Romanov, and R. Z. Valiev, "On the structure, stress fields and energy of nonequilibrium grain boundaries," *Acta Metallurgica et Materialia*, vol. 41, pp. 1033-1040., 1993.
[38] J. W. Christian, "Some surprising features of the plastic-deformation of body-centered cubic metals and alloys," *Metallurgical Transactions A*, vol. 14, pp. 1237, 1983.
[39] A. M. Lennon and K. T. Ramesh, "The thermoviscoplastic response of polycrystalline tungsten in compression," *Materials science and engineering A*, vol. 276, pp. 9-21, 2000.
[40] T. Dummer, J. C. Lasalvia, G. Ravichandran, and M. A. Meyers, "Effect of strain rate on plastic flow and failure in polycrystalline tungsten," *Acta materialia*, vol. 46, pp. 6267-6290, 1998.
[41] P. J. Blau, R. L. Martin, and E. S. Zanoria, "Effects of surface grinding conditions on the recprocating friction and wear behavior of silicon nitride," *Wear*, vol. 203, pp. 648-657, 1997.
[42] D. Tabor, *The hardness of metals*. Oxford: Clarendon Press, 1951.
[43] A. S. Argon and S. R. Maloof, "Plastic deformation of tungsten single crystals at low temperature," *Acta Metallurgica*, vol. 14, pp. 1449-1462, 1966.
[44] T. Watanabe, "An approach to grain boundary design for strong and ductile polycrystals," *Res Mechanica*, vol. 11, pp. 47-84, 1984.
[45] R. Z. Valiev, I. V. Alexandrov, Y. T. Zhu, and T. C. Lowe, "Paradox of strength and ductility in metals processed by severe plastic deformation," *Journal of Materials research*, vol. 17, pp. 5--8, 2002.
[46] P. Gumbsch, J. Riedle, A. Hartmaier, and H. F. Fischmeister, "Controlling factors for the brittle-to-ductile transition in tungsten single crystals," *Science*, vol. 282, pp. 1293-1295, 1998.
[47] T. W. Wright, *The physics and mathematics of adiabatic shear bands*: Cambridge Press, 2002.

NO. OF
COPIES ORGANIZATION

1 (PDF ONLY) DEFENSE TECHNICAL INFORMATION CTR
DTIC OCA
8725 JOHN J KINGMAN RD
STE 0944
FORT BELVOIR VA 22060-6218

1 US ARMY RSRCH DEV & ENGRG CMD
SYSTEMS OF SYSTEMS INTEGRATION
AMSRD SS T
6000 6TH ST STE 100
FORT BELVOIR VA 22060-5608

1 INST FOR ADVNCD TCHNLGY
THE UNIV OF TEXAS
AT AUSTIN
3925 W BRAKER LN
AUSTIN TX 78759-5316

1 DIRECTOR
US ARMY RESEARCH LAB
IMNE ALC IMS
2800 POWDER MILL RD
ADELPHI MD 20783-1197

3 DIRECTOR
US ARMY RESEARCH LAB
AMSRD ARL CI OK TL
2800 POWDER MILL RD
ADELPHI MD 20783-1197

ABERDEEN PROVING GROUND

1 DIR USARL
AMSRD ARL CI OK TP (BLDG 4600)

NO. OF
COPIES ORGANIZATION

ABERDEEN PROVING GROUND

6 DIR USARL
AMSRD ARL WM
R DOWDING
AMSRD ARL WM MB
K CHO
L KECSKES
AMSRD ARL WM TC
R COATES
L MAGNESS
B SORENSEN